7 Electromagnetic Fields in Relation to Cardiac and Vascular Function

Harvey Mayrovitz

CONTENTS

INTRODUCTION

In considering the role of electromagnetic fields (EMFs) as applied to cardiac function, there are several broad roles open for contemplation. One is the use of EMF to provide cardiac monitoring and diagnostic information not easily obtainable via other methods. This aspect relies on the magnetic field produced by the heart being detectible and signals so detected to provide functional information regarding cardiac status. One example is the measuring of fetal heart rate (HR) parameters (Moraes, Murta et al. 2012, Van Hare 2013, Wacker-Gussmann, Paulsen et al. 2014, Batie, Bitant et al. 2018), a procedure not easily done with standard methods. Another example would be the measuring of physiological parameters such as cardiac volume changes via magnetic susceptibility changes (Wikswo 1980, Wikswo, Opfer et al. 1980, Roth and Wikswo 1986).

A second category of potential and possible use of EMF is as a treatment modality for cardiac dysfunction. Such dysfunction may include HR or rhythm disorders

or disorders related to cardiac blood flow inadequacy or cardiac muscle dysfunction (Yuan, Wei et al. 2010, Li, Yuan et al. 2015).

A third category of potential applications of EMF is cardiac protection. This relates to how exposure to suitable magnetic fields might reduce risk of future cardiac dysfunction. Examples may include reduction of blood viscosity with pulsed electromagnetic fields (PEMFs)(Tao and Huang 2011, Tao, Wu et al. 2017) as a way to diminish vascular resistance, the use of PEMF to increase cardiac endothelial cell proliferation (Li, Yuan et al. 2015), or the use of bioelectromagnetic actions to reduce blood pressure (Tasic, Djordjevic et al. 2017).

A fourth general category of cardiac–biomagnetic interaction relates to unintended or uncontrolled cardiac effects caused by external sources. Examples may include potential cardiac effects associated with electromagnetic therapy applied to other body parts (Yoshida, Yoshino et al. 2001, Wang, Hensley et al. 2016) or even changes in the geomagnetic field (McCraty, Atkinson et al. 2017, Jarusevicius, Rugelis et al. 2018, Žiubrytė, Jaruševičius et al. 2018a,b).

EMF approaches, devices, and methods that relate to its potential utility in the mentioned categories have been proposed and evaluated and, in some cases, have demonstrated functional utility for detection and treatment. Although, some approaches and methods have theoretically sound foundations, some may not have yet been applied or even evaluated. The main purpose of this chapter is to offer a framework from which past, present, and possible future EMF applications related to cardiac and vascular function may be appreciated in the context of the associated physiological and pathophysiological underpinnings.

MONITORING CARDIAC FUNCTION UTILIZING THE HEART'S MAGNETIC FIELD

Physiological Processes

Cardiac transmembrane ionic currents associated with myocardial depolarization and repolarization sweep through the heart causing it to contract and then relax resulting in blood pumping and refilling, respectively. Electrical potential changes (action potentials, APs) associated with these waves of depolarization and repolarization are caused by Na^+, K^+, and Ca^{++} ion movements across cardiac cell membranes through specific ion channels. The current and AP changes are sensed by surface electrodes to generate the well-known electrocardiogram (ECG). A typical ECG pattern has a P-wave associated with atrial contraction, a QRS complex associated with ventricular depolarization, and a T-wave associated with ventricular repolarization (Figure 7.1). The initiation of this electrical activity normally starts at the sinoatrial node (SAN) located in the right atrium. It spontaneously depolarizes and acts as the heart's pacemaker. The ventricles have electrical activity during the QT interval (Figure 7.1) but are electrically quiet during the TQ interval. The AP associated with ventricular myocytes and conduction fibers is divided into phases (ϕ) with ϕ_4 being the resting phase, ϕ_0 a rapid depolarization phase that is mainly associated with a rapid influx of Na^+, a ϕ_2 plateau phase involving Ca^{++} influx and K^+ efflux, and ϕ_3 a repolarization phase in which Ca^{++} influx is diminished and counterbalanced by

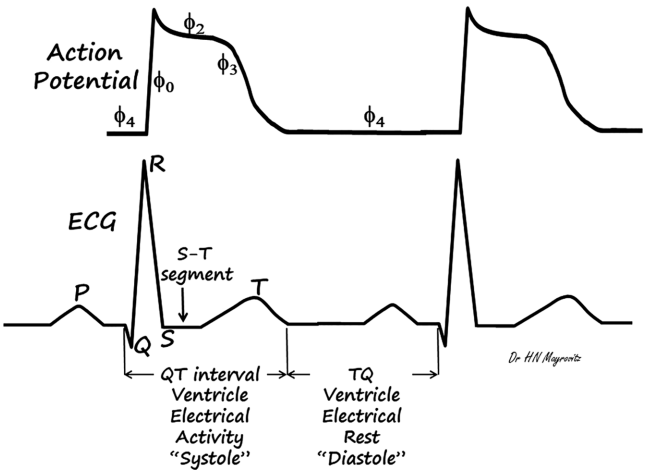

FIGURE 7.1 A cardiac ventricular action potential (AP) and a corresponding electrocardiogram (ECG) showing the waves and time correlation between the AP and the ECG. Ventricular electrical activity occurs during the QT interval. The phases (ϕ) of the AP are indicated.

K^+ efflux. Depolarization and repolarization currents are quite small but give rise to magnetic fields that can be sensed by suitable devices. The ECG is used to estimate the mean QRS electric vector to help diagnose ventricular hypertrophy and other conduction abnormalities. The ECG vector (mean electrical axis) is reported similar to the direction of the magnetic vector (Barry, Fairbank et al. 1977).

The Cardiac Magnetic Field

Magnetic fields due to cardiac currents are very small, in the neighborhood of 1 nT if measured close to the heart surface(McBride, Roth et al. 2010) and about 0.1 nT at the body surface (Geselowitz 1973). Despite such small magnitudes, Stratbucker and coworkers were able to use a toroidal solenoid containing 17,640 turns to successfully detect cardiac generated fields that were in time synchrony with ECGs obtained from isolated guinea pig hearts (Stratbucker, Hyde et al. 1963). Their estimated value for the magnetic dipole moment of the QRS complex was in good agreement with measured values.

The first measurements on nonisolated hearts appear to have been made by Baule and McFee employing two multiturn coils (2×10^6 turns) over the chest (Baule and McFee 1963). Using this method, it was determined that the voltage induced in the coil (v) depends on the number of turns (n), the permeability of the core (μ), the loop cross-sectional area (A), and the angle (θ) that the loop axis makes with respect to magnetic field strength vector **H**.

The detected voltage is approximately $v = n\mu\cos(\theta)d\mathbf{H}/dt$. Since H is a vector, its full simultaneous specification would require the use of three mutually orthogonal coils (Geselowitz 1979). Due to extraneous signals, even in magnetically shielded areas, the signal to noise ratio can be a limitation in obtaining consistently reliable

data. Such measurements now are most often done with a superconducting quantum interference device (SQUID) used in adult (Fujino, Sumi et al. 1984) and in fetal (Zhuravlev, Rassi et al. 2002) applications to obtain magnetic counterpart of the ECG called the magnetocardiogram (MCG). An example of the ECG–MCG correspondence is shown in Figure 7.2 that is drawn based on and representative of values of Brockmeier and colleagues (Brockmeier, Schmitz et al. 1997).

Detection of the magnetic field associated with cardiac currents can be a useful adjunct to other diagnostic monitoring methods. Assessment methods using simulations indicate that the magnetic field associated with cardiac repolarization APs is greater than that which would be predicted simply based on considerations of time rates of change of transmembrane potentials (Barach and Wikswo 1994). This observation suggests involvement of other factors. Some such factors examined relate to the extent to which changes in the conductivity of cardiac tissue and blood might affect the measured external field. Further simulation results suggest that changes in blood and myocardium conductivity are importantly involved (Czapski, Ramon et al. 1996). But, given the long history of the ECG as an immensely useful diagnostic tool, the use of MCG might at first glance be questionably redundant. However, arguments have been made suggesting otherwise.

It has been suggested that there is information within the MCG signal that is not available in the ECG signal. One aspect of this difference may relate to the fact that the ECG detects cardiac electrical activity as a flux source but the MCG detects it as a vortex source (Plonsey 1972). Furthermore, some theoretical work supports the concept of basic informational differentials between electric and magnetic sensing (Roth and Wikswo 1986). An example of this in the heart relates to the fact that in certain myocardial regions, because of the anatomical arrangement of muscle fibers, some cardiac currents contribute to the ECG, but some do not. The currents that do

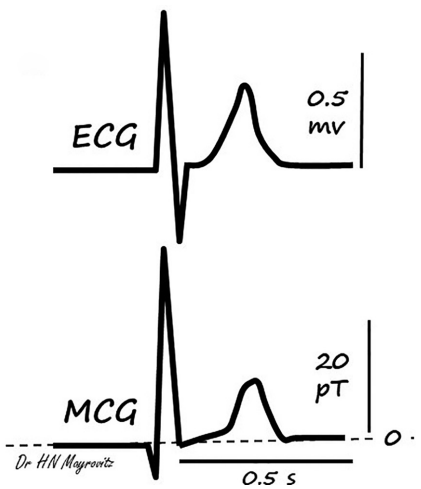

FIGURE 7.2 Illustrating the similarity between the pattern of a measured ECG and magnetocardiogram (MCG).

not contribute to the ECG would however be detectible via the MCG, thus yielding additional information. Measurements using SQUID in rabbit hearts (McBride, Roth et al. 2010) were felt to be consistent with this concept. The value of such added information in a clinical setting remains to be established.

There are other aspects to be considered when comparing potential utilities of MCG versus ECG. MCG signals do not require skin contact and are much less affected by the electrical conductivity of tissues and fluids that lie between heart and skin surfaces than ECG signals. MCG is also useful for a variety of fetal cardiac evaluations as shown for fetal tachycardia (Abe, Hamada et al. 2005), changes in the fetal QRS complex (Horigome, Takahashi et al. 2000), characterizing accessary pathway features (Kandori, Hosono et al. 2003), fetal third degree block (Hosono, Shinto et al. 2002), fetal atrial fibrillation (Kandori, Hosono et al. 2002), and, more recently, significant advancements in detecting a variety of fetal arrhythmias (Stingl, Paulsen et al. 2013, Yu, Van Veen et al. 2013, Kiefer-Schmidt, Lim et al. 2014, Wacker-Gussmann, Paulsen et al. 2014). In other applications, the potential advantage of MCG versus ECG in detecting the dominant frequency of atrial fibrillation in adults has also been reported (Yoshida, Ogata et al. 2015). Other cardiac conditions for which MCG has demonstrated potential utility above that offered by standard ECG include detecting certain abnormalities associated with ischemic heart disease (Watanabe and Yamada 2008), improved prediction of future major cardiac events in patients with dilated cardiomyopathy (Kawakami, Takaki et al. 2016), and other cardiac conditions (Gapelyuk, Wessel et al. 2007, Schirdewan, Gapelyuk et al. 2007, Van Leeuwen, Hailer et al. 2008, Gapelyuk, Schirdewan et al. 2010).

In addition to potential direct clinical applications of MCG, there appears to be room for its use to study and uncover physiological and pathologic features not easily discoverable via ECG data. A beautiful example is to be found in the pioneering work of Cohen and coworkers who studied the mechanism and underlying aspects of the now well-known shift in the ECG S-T segment that occurs with cases of STEMI myocardial infarction (Loomba and Arora 2009). At the time, details of such shifts were unclear. It was reasoned that one possibility was that the shift was caused by cardiac currents flowing only during the S-T segment interval and that those currents arose due to regional differences in membrane APs. This possibility was termed "primary shift" or "true shift". The other possibility was that the observed S-T segment shift was due to the presence of a continuous steady injury current that was interrupted only during the S-T interval. This was termed "secondary shift" or apparent shift". Part of this process is shown in Figure 7.3 that shows conditions during the ventricular electrical resting phase (during the ECG T-Q interval).

In part A of Figure 7.3, the membrane potentials between normal myocytes are not different in magnitude (negative inside with respect to outside), so the potential difference between them is zero. If some cells become ischemic, as shown in part B, reduced O_2 available to their Na^+–K^+ pumps results in diminished pump function causing partial depolarization of these cells. This gives rise to a potential gradient between normal and ischemic cells that becomes a source of an "injury current".

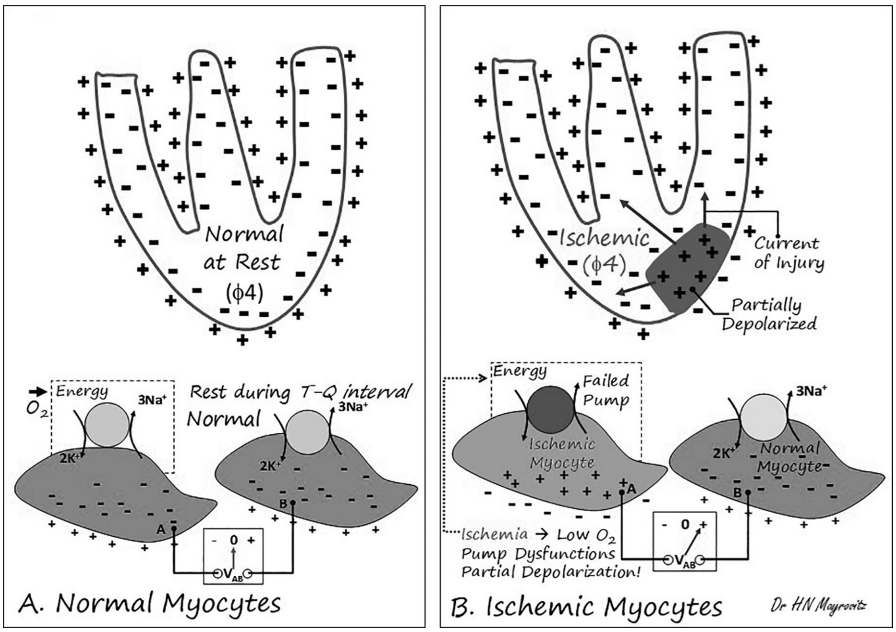

FIGURE 7.3 Illustrating the change in cardiac cellular transmembrane potentials induced by ischemia. In (A) is shown normal healthy cells and in (B) is shown what can happen when one of the cells (or regions) becomes ischemic. The low oxygen alters the cell's sodium-potassium pump function causing a difference in electrical potential between healthy and ischemic cells. Such potential differences can give rise to so-called injury currents.

The direction of the injury current depends on the phase of the cardiac AP under consideration as illustrated in Figure 7.4.

In Figure 7.4, a region of the ventricular wall near the endocardium is assumed to experience an inadequate blood flow (ischemia). The reduced availability of O_2 causes partial depolarization of the ischemic cell's resting AP that also has a reduced amplitude as shown dotted in the figure. The S-T segment of the ECG occurs during ventricular systole. During this time, current flow is from normal cells to ischemic cells as indicated. However, during ventricular diastole (T-Q interval of Figure 7.1), an injury current would flow from ischemic to healthy cells. The use of MCG to study this process was first determined in dogs (Cohen, Norman et al. 1971, Cohen and Kaufman 1975) followed by measurements in humans (Cohen, Savard et al. 1983, Savard, Cohen et al. 1983) using SQUID measures.

An illustrative example of the evolution of S-T segment shifts with exercise, as investigated using MCG, is shown in Figure 7.5 drawn based on the data of Cohen, Savard et al. (1983). Results from the dog experiments implicated an initial acute ischemia-related induction of a steady "injury current" that was then interrupted via depolarization during the S-T interval. This would correspond to part-labeled "systole" in Figure 7.4. This process gave rise to the visualized S-T segment shift that

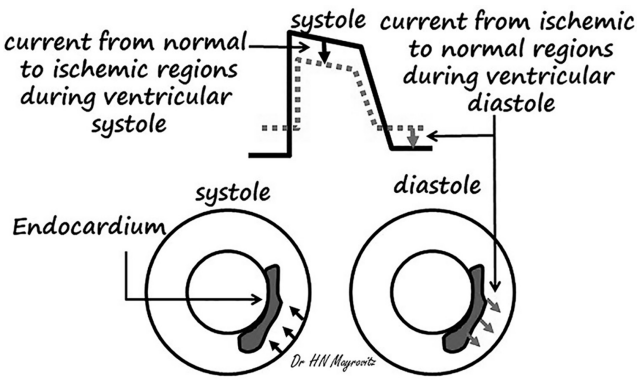

FIGURE 7.4 Illustrating the directional changes in injury currents associated with a region of myocardial ischemia that depends on the time interval of the cardiac action potential. The time interval labeled "systole" is associated with the electrically active QT interval. The interval labeled "diastole" is associated with the quiescent TQ interval.

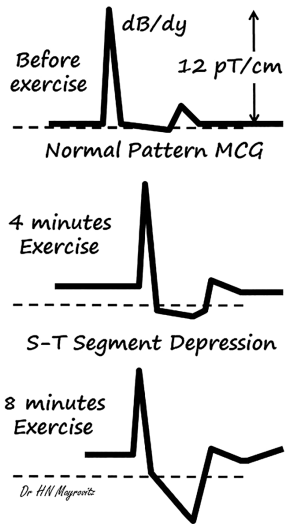

FIGURE 7.5 Illustrating the progressive changes in an MCG associated with evolving ischemia.

would be considered "secondary" according to the nomenclature of these authors. After this initial change, there seemed to be a transition to a true S-T segment shift.

However, in using MCG to study S-T segment shifts in a person with a left bundle branch block (LBBB) and in three persons with early repolarization (ER) syndrome (Savard, Cohen et al. 1983), the magnetic data showed no evidence of

a continuous current baseline shift. In these conditions, a "primary shift" mechanism was assumed to be the main cause. For the three persons with ER, the explanation for the shift would be that abnormally early repolarization in some myocardial regions causes a voltage gradient that drives current between those regions. This current would start during the early part of phase 3 and would closely correspond to the abnormal currents shown in Figures 7.3 and 7.4 but would not require an ischemic basis. The S-T segment shift the authors observed in the patient with LBBB may also be accounted for on the basis of regional differences in repolarization, not due ischemia but instead due to delayed conduction causing a right-to-left voltage gradient during repolarization. Subsequent evaluation of a person with coronary artery disease undergoing stress testing indicated that an ischemia-dependent S-T segment depression (of which Figure 7.5 is representative) is related to both true and apparent mechanisms (Cohen, Savard et al. 1983).

The details herein provided concerning these prior studies helps visualize the potential for MCG measurements. It is noteworthy that most of these and other experimental observations and conclusions would not have been possible without the unique ability of the MCG to measure direct current (DC) fields and their changes, a feature not possible with an ECG. However, the fact that DC measurements are possible means that low-frequency filtering is not applicable, thereby increasing the risk of external interference. In addition, signals arising due to DC fields originating in other organs (e.g., the gastrointestinal system) need to be considered in any analysis and interpretive process of any composite MCG signal.

Some progress has been made in utilizing modalities other than SQUID systems to detect MCG-related information. One example is the use of arrays of magnetoresistive sensors that respond to external cardiac magnetic fields by changing their resistance. A pilot study indicated the possibility of detecting P, QRS, and T waves if suitable averaging methods are used (Shirai, Hirao et al. 2018). Another type of potential advance in the field relates to enhanced processing of acquired MCG signals that offer the possibility for improved diagnosis and characterization of adult ischemic heart disease based on MCG features (Tao, Zhang et al. 2018) and on processing of fetal MCG data (Escalona-Vargas, Wu et al. 2018).

Other advancements in the use of MCG parameters have focused on developing scoring systems with associated threshold values to better characterize and detect coronary artery disease with adequate positive and negative predictive levels (Shin, Park et al. 2018a,b). Partly because standard MCG utilization usually requires enhanced room shielding for proper operation the widespread use of this technology for research and clinically related applications has been limited. Other emerging approaches have evaluated the possibility of MCG use in nonshielded environments using repeatability measures of various MCG-related parameters (Sorbo, Lombardi et al. 2018). However, the use of multichannel MCG remains an evolving methodology as demonstrated by the recent report of its use in detecting patients at high risk for lethal arrhythmias (Kimura, Takaki et al. 2017) and its reported increased discriminating ability compared to ECG to characterize cardiac repolarization features (Smith, Langley et al. 2006).

CARDIAC IMPACTS AND APPLICATIONS OF APPLIED BIOMAGNETIC FIELDS

When considering impacts of applied PEMF on cardiac parameters, there are two general categories to consider. One relates to the heart's exposure to fields that are not specifically directed toward affecting heart parameters but cause changes as "side effects". This includes potential effects of transcranial magnetic stimulation (TMS) and fields associated with magnetic resonance imaging (MRI) (Chakeres, Kangarlu et al. 2003). The other general category relates to specific targeted applications that are designed to alter cardiac parameters to treat cardiac arrhythmias and other aspects of dysfunction. In each category, an applicable concept is one of an approximate magnetic dipole of current source **I** amps in a coil of area A. For such a dipole at some distance (r) from the biological target, $\mathbf{H}(r,\theta) = [\mathbf{m}/4\pi r^3]\ (1 + 3\cos^2\theta)^{1/2}$. In this equation, **m** is the coil's dipole magnetic moment (**I**A), and θ is the angle with respect to its axis.

Calcium Currents as a Target

The way in which such fields may produce their cardiac effects is unclear. However, it is known that calcium dynamics play multiple roles in relation to cardiac electrical and mechanical properties and function, and there is widespread data demonstrating bioelectromagnetic-Ca^{++} interactions (Smith, McLeod et al. 1987, Blackman, Benane et al. 1988, Walleczek and Budinger 1992, Pilla, Muehsam et al. 1999, Coulton, Barker et al. 2000, Zhao, Yang et al. 2008, Muehsam and Pilla 2009, Lu, Du et al. 2015). Thus, it is likely EMF-Ca^{++} linkages are also involved in cardiac cellular aspects.

Experimental work with the frog heart model has suggested a potential frequency and intensity window that can alter Ca^{++} dynamics (Schwartz, House et al. 1990). The increase in Ca^{++} efflux from hearts exposed to 240 MHz modulated at 16 Hz showed these effects, but the effects were not observed when unmodulated or modulated at 0.5 Hz. Other effects, reported when electrical and mechanical features were recorded during SMF exposure (0.34–1.56 T), included rate irregularities and reductions in contraction force and diastolic relaxation (Reno and Beischer 1966). Whether these changes are related to Ca^{++} dynamics is not verified, but it is clear that all observed physiological changes could be linked to Ca^{++} dynamics.

Although frog hearts do not depend on Ca^{++} release from sarcoplasmic reticulum for contraction as human heart does, reduction in free Ca^{++} during systole and reduced reuptake of cytosol Ca^{++} during diastole could explain the reduced contraction force and reduced diastolic relaxation observed. Further, the electrical rhythm changes might be explained by altered sinus node diastolic depolarization features associated with field-induced Ca^{++} changes. In part, motivated by these and other observations, several innovative ideas have been put forward broadly describing noninvasive ways to impact cardiac function and arrhythmias (Laniado, Kamil et al. 2005, Kassab, Navia et al. 2013, Scheinowitz, Nhaissi et al. 2018).

It was noted earlier that there is some evidence that geomagnetic field variations might be associated with various cardiac-related dysfunctions including myocardial

infarction (Jarusevicius, Rugelis et al. 2018), atrial fibrillation (Žiubrytė, Jaruševičius et al. 2018), and angina pectoris (Žiubrytė, Jaruševičius et al. 2018). It is possible to speculate that such correlations are related to the fact that the excitation frequency for cardiac cell Ca^{++} transient currents depends on small variations in a copresent DC magnetic field ranging from about 44 to 49 μT (Fixler, Yitzhaki et al. 2012).

Transcutaneous Magnetic Stimulation (TMS)

Transcutaneous magnetic stimulation (TMS) is a rapidly growing electromagnetic application and, as the name implies, is the use of PEMF to stimulate brain tissue with applicator coils placed on the scalp surface. This allows the magnetic field to pass through the skull to the brain tissue region of interest. Because in some cases there are a series of pulses associated with the treatment, it is further characterized as repetitive TMS or simply rTMS as compared to a single pulse treatment modality (sTMS). One early treatment target for this modality was depression that received FDA clearance in 2008. For this condition, a series of 20–25 treatments over 4–6 weeks has been used by some practitioners. Although reported to be effective for a variety of conditions, there has been concern as to its possible impacts on cardiac function. Some workers have reported associated cardiac changes. These include increased HR and a possible shift in the balance between parasympathetic and sympathetic activity (Cabrerizo, Cabrera et al. 2014) and other heart-rate related effects when using rTMS to treat autistic children (Wang, Hensley et al. 2016). Since it appears that the clinical use of TMS is expanding, it is likely that further cardiac impacts will be discovered.

Magnetic Resonance Imaging (MRI)

A second source of cardiac exposure to bioelectromagnetic fields is associated with the use of MRI for diagnostic purposes. Static magnetic fields (SMFs) associated with such MRI systems now include 1.5 T, 3.0 T, and the increasing use of 7 T devices that permit better resolution than lower-intensity devices(Park, Kang et al. 2018). These higher intensities may be especially useful for the assessment of brain small vessel disease (Geurts, Bhogal et al. 2018, Geurts, Zwanenburg et al. 2018). Future applications of the 7 T field are likely to provide improved resolution in spinal cord (Barry, Vannesjo et al. 2018), breast (Li and Rispoli 2019), peripheral nerves(Yoon, Biswal et al. 2018), quantifying cerebral spinal fluid movement (Markenroth Bloch, Toger et al. 2018), and a variety of other applications (Barisano, Sepehrband et al. 2018). Given this situation, it is natural to consider the possible effect of these high field intensities on cardiac-related parameters. One report has indicated that exposure to an SMF of 2 T reduces resting HR during the first 10 min of exposure (Jehenson, Duboc et al. 1988), but that HR is subsequently normalized. Assessment of HR changes in squirrel monkeys in response to exposure to 7 T fields for about an hour has also shown HR reductions (Beischer and Knepton 1964). Contrastingly, other studies (Chakeres, Kangarlu et al. 2003) have indicated no effect of MRI-generated static fields measured with intensities ranging from 0.8 to 8.0 T. The question of impacts of high-intensity fields on cardiac parameters remains unclear.

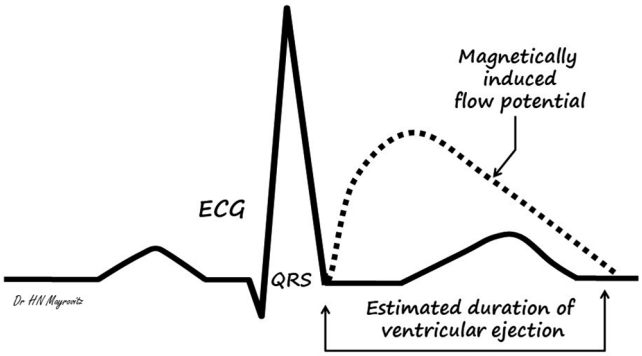

FIGURE 7.6 Illustrating the timing of a magnetically induced flow potential associated with blood flow interacting with an intense static magnetic field.

Magnetohemodynamic Considerations

An additional consideration with respect to high-intensity applications is the potential impact that occurs due to interactions between applied magnetic fields and blood hemodynamics. Movement of blood within a static field gives rise to a generated electrical potential, a process that forms the basis of electromagnetic blood flow measurement in large blood vessels (Kolin, Assali et al. 1957). Impacts of such externally applied fields have been considered as they affect blood flow in larger arteries (Chen and Saha 1984, Okazaki, Maeda et al. 1987, Sud and Sekhon 1989, Kinouchi, Yamaguchi et al. 1996) and blood and blood flow in small blood vessels (Takeuchi, Mizuno et al. 1995, Higashi, Asjoda et al. 1997, Haik, Pai et al. 2001, Bali and Awasthi 2011). However, the possible role of a magnetically induced voltage affecting cardiac function has not been clarified. Such a generated voltage, termed "flow potential", was initially observed on ECG recordings made when squirrel monkeys were exposed to static magnetic fields ranging from 4 T to 10 T (Beischer and Knepton 1964). This flow potential measured at the skin surface was about 0.5 mv and was estimated to be about 100 mV when extrapolated back to the heart.

An interesting feature of this flow potential was that it appeared to occur maximally during ventricular ejection and thereby might be useable as an index of ascending aortic blood flow as schematically illustrated in Figure 7.6. Whether or not this induced potential would serve as an ectopic impulse to produce cardiac arrhythmias likely depends on its magnitude and timing. As illustrated in Figure 7.6, the flow potential occurs during a time interval when most of the ventricular myocardium is refractory. However, it could have an impact on atrial cells.

Heart Rate Variability (HRV)

Several studies have examined the potential impact of magnetic fields associated with MRI on HRV parameters. The significance of HRV is in part related to its characterization of cardiac status as determined by the sympathetic–parasympathetic balance controlled by the autonomic nervous system (ANS). This relationship is

based on the fact that sympathetic and parasympathetic (vagus) nerve traffic to the sinoatrial node largely determines HR changes measured as variations in ECG R–R intervals. Thus, HRV may be broadly viewed as a neurocardiac process (Shaffer and Ginsberg 2017), and its complexity should be kept in mind (Pagani, Lombardi et al. 1986) when interpreting changes.

Since vagus control can effectuate more rapid changes in HR than sympathetic control, the higher-frequency spectral components of the interbeat time series (R–R intervals) are considered to represent parasympathetic activity and the lower-frequency components viewed as being indices of sympathetic activity. For spectral analysis purposes, the ratio of high-frequency power to low-frequency power is taken as an index of the balance between parasympathetic and sympathetic activity. A higher ratio would be considered good from a cardiovascular perspective. Similarly, for time-domain analyses, a greater HRV as determined by the variance of consecutive R–R intervals is considered good from a cardiovascular perspective. In fact, most studies indicate a reduction in HRV as predictive of negative cardiovascular morbidity and mortality outcomes. However, in some conditions, it appears that an increase in certain HRV temporal parameters are predictive of vascular decline as in the progression of small blood vessel disease in elderly persons (Yamaguchi, Wada et al. 2015). Intracardiac conduction abnormalities can also lead to increased HRV, so increases should not always be interpreted as "good".

Effects of diagnostic MRI (1.5 T) on HRV of 42 patients indicated an increase in HRV as determined by increased R–R interval standard deviations (SDs) (Derkacz, Gawrys et al. 2018). In another study, a 30 min MRI exposure with a 1.5 T field was also associated with increases in time-domain HRV parameters as well as increases in all spectral components (Sert, Akti et al. 2010). However, the potential impacts of MRI procedural anxiety on HRV changes (Pfurtscheller, Schwerdtfeger et al. 2018) should be considered in all such comparisons. A report (Ghadimi-Moghadam, Mortazavi et al. 2018) concerning effects of a relatively low-intensity MRI (1.5 T) on staff workers and test subjects suggests that further research is needed especially in light of the pending increasing use of higher-power units. It is noteworthy that short intervals of head exposure to low-intensity static fields (200 μT) (Koppel, Vilcane et al. 2015) and short- and long-time (12 h) whole body exposure to extremely low-frequency (ELF 50–1,000 Hz) at 100 μT (Kurokawa, Nitta et al. 2003) did not significantly alter any HRV parameter. However, there is now some evidence that environmental magnetic fields associated with Schumann resonance power changes can increase HRV with associated increases in parasympathetic activity (Alabdulgader, McCraty et al. 2018).

POTENTIAL CARDIAC AND VASCULAR TARGETS OF BIOELECTROMAGNETIC THERAPY

Cardiac Arrhythmias

Normally, HR is controlled by actions within the sinoatrial node (SAN) located in the right atrium. Its function depends strongly on actions of a so-called ionic "funny" current, I_f, (DiFrancesco, 2010) which if increased causes HR to increase and if decreased causes HR to decrease. Although normal SAN pacemaker activity

can operate independently of the ANS, the SAN is richly innervated, and its activity is modulated by nerve traffic from both sympathetic and parasympathetic nervous systems. Increased sympathetic activity acts on β-adrenergic receptors causing I_f to increase thereby increasing HR. Contrastingly, increased parasympathetic activity via the vagus nerve acts on muscarinic receptors and causes I_f and also HR to decrease. Acetylcholine (Ach) is the neurotransmitter involved in the slowing of the HR by the vagus and is rapidly degraded via the action of acetylcholinesterase (AChE), thereby rendering vagus control responsible for handling higher rates of change in HR.

Recognizing the importance of Ach and AChE, Wei Young developed a frog (*Rana pipiens*) vagal heart model that, among other uses, could be exposed to a magnetic field with subsequent effects being observed and described (Young 1969). Exposure to a static field of 0.27 T resulted in an increase in the hydrolysis of ACh and increased AChE activity. These changes caused the duration of vagal inhibition of the SAN to be lessened. However, when the field was increased to 1.0 T, arrhythmias were often detected. Based on multiple observations, it was speculated that the magnetic field was producing a conformational change in enzyme molecules at low intensity but damage at higher intensity. The precise explanation for these HR effects remains absent, but observations points out the complexity involved in these processes. Figure 7.7 illustrates a reported effect of a 10 pT excitation field at 16 Hz obtained from a pig model and herein drawn based on prior data (Laniado, Kamil et al. 2005). As illustrated, the effect was to increase HR and reduce the PR interval measured on the ECG. Although the mechanisms causing these changes are not defined, the fact that such changes can occur rapidly (within 2 min of application) provides experimental data from which to pursue and investigate such issues.

Under some circumstances, the normal pacing actions are lost when the electrical activity of the atrium becomes chaotic with different parts of the atrium depolarizing rapidly and randomly. One form of this chaotic activity is atrial fibrillation (AF) that is the most widely experienced sustained cardiac arrhythmia (Ellervik, Roselli et al. 2019,

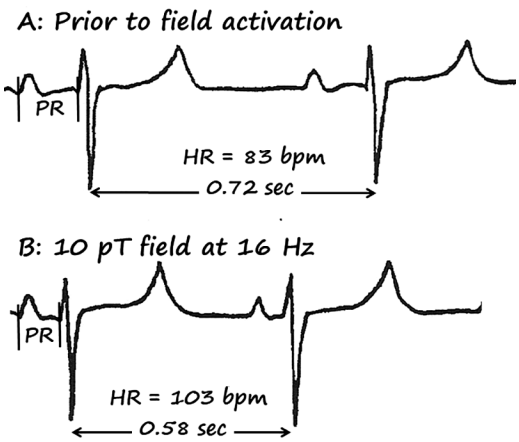

FIGURE 7.7 Illustrating an effect of a 16 Hz field on heart rate and atrial-to-ventricle conduction.

Roberts 2019, Salem, Shoemaker et al. 2019). AF is thought to occur as a consequence of interactions between initiating electrical triggers that impact cardiac tissue that is susceptible to allowing such triggers to cause AF. The resultant AF can be transient and rapidly self-terminating or persistent in need of treatment (medicine or cardioversion or ablation) or a permanent type that is unresponsive to treatment. Ablation treatment, which is invasive, is reported to be 60%–70% effective (Woods and Olgin 2014).

In contrast to invasive interventional procedures, some workers have suggested the use of noninvasive approaches that target the ANS as a way to treat AF and other cardiac arrhythmias (Li, Zhou et al. 2015). The ANS is theorized to be a target for such intervention because of its potential role as a trigger for AF. This being partly related to a β-adrenergic effect that can cause an increase in myocardial automaticity or promote ectopic focal impulses of either the early afterdepolarization (EAD) or delayed afterdepolarization (DAD) types (Chen, Chen et al. 2014). Parasympathetic factors may also be involved (Liu and Nattel 1997).

The neural influences of both sympathetic and parasympathetic nerves on cardiac electrical activity is largely dependent on their interaction with ganglionated plexi that are mostly imbedded in fat pads lying on atrial and ventricular epicardial surfaces (Pauza, Skripka et al. 2000). These plexi contain sympathetic and parasympathetic components with afferent, efferent, and interconnecting neurons (Stavrakis and Po 2017) and are likely involved in initiation and maintenance of AF (Nishida, Datino et al. 2014). Various approaches are there in the medical arsenal to treat this condition, but stoppage of the atrial fibrillation in theory might occur if the atrium, in which these chaotic circulating depolarizations are present, could be rendered transiently refractory, thereby snuffing out the arrhythmia via the application of bioelectromagnetic energy of the proper configuration. An example of an externally applied magnetic field signal, derived from adding together single cycles of two different sinusoidal signals, has been proposed to serve as a leadless magnetic cardiac pacemaker. One form of a signal, shown in Figure 7.8, has been claimed to stabilize

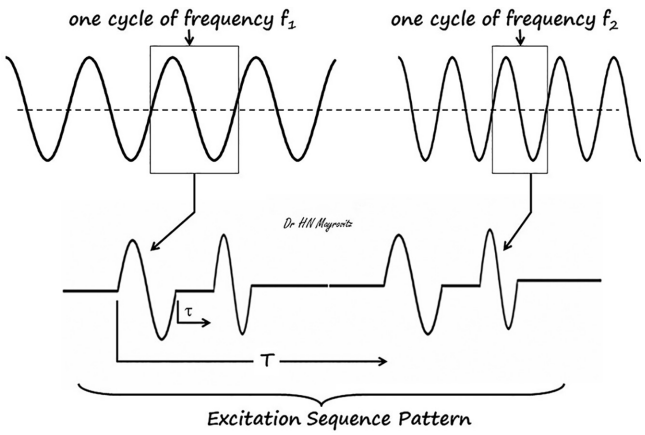

FIGURE 7.8 Illustrating the synthesis of a complex excitation pattern based on the addition of single cycles of differing frequency.

an erratic heartbeat as assessed in an isolated canine heart (Ramon and Bardy 1992). As drawn herein, the parameters τ and T are subject to variation to best match target tissues. This needs to be done empirically. This pattern is of course but one of many possible signal patterns that may impact biological activity.

Cardioprotection

The possibility that exposure to low-intensity PEMF could reduce the negative effects of experimental myocardial infarction (MI) was carefully investigated using a rat model (Barzelai, Dayan et al. 2009). Following ligation of the left anterior descending artery, rats were housed either in cages in which the floor was composed of 69 current loops that generated a 16 Hz field of 80–100 nT at their heart level or in nonfield exposed enclosures. Assessment of cardiac function 4 weeks post MI induction showed a greater shortening fraction in rats exposed to the magnetic field and more blood vessels in surviving tissues of the 4-week remodeled myocardium (Barzelai, Dayan et al. 2009). It is unclear if the reported protective effect was related to the increased small blood vessel density.

There is other evidence that exposure to PEMF is more generally associated with angiogenic processes in experimental animals rendered ischemic(Pan, Dong et al. 2013), but it can be stimulatory or inhibitory (Strelczyk, Eichhorn et al. 2009, Wang, Yang et al. 2009, Markov 2010, Delle Monache, Angelucci et al. 2013) possibly dependent on applied field frequency and intensity. For example, a 60 Hz, 2 mT field is reported to diminish new vessel formation potentially through downregulation of the vascular endothelial growth factor (VEGF) pathway (Delle Monache, Angelucci et al. 2013). However, cardioprotective results were also shown for rats in which the left coronary artery had been ligated. Cardiac capillary density 4 weeks post ligation measured in rats treated with 15 Hz fields (6 mT) for 3 h/day was significantly greater than in both rats not treated and those treated at 10 Hz (Yuan, Wei et al. 2010). An accompanying differential elevation in VEGF may have been involved in this process. Furthermore, rats treated with 15 Hz fields had less infarct size and had better cardiac function assessed via maximal rate of change of ventricular pressure. In part based on such findings in experimental animals, various devices have been proposed as ways to promote cardiac angiogenesis, with one approach illustrated in Figure 7.9 based on one of several embodiments in a 2001 patent (March 2001).

In searching for mechanisms, it was hypothesized that myocyte protection may be due to a PEMF-related opening of adenosine-triphosphate-activated potassium channels (K_{ATP}) (Barzelai, Dayan et al. 2009, Fixler, Yitzhaki et al. 2012, Aharonovich, Scheinowitz et al. 2016). These channels are present in myocyte sarcolemma, but most are normally not open (Nichols, Singh et al. 2013). However, reduced blood flow can open these channels causing increased outward K^+ flux. This produces a cellular hyperpolarization and a more rapid AP repolarization. This in turn reduces the action potential duration (APD) and also reduces Ca^{++} entry into the myocyte thereby reducing myocardial contractility. This would conceptually provide a temporary energy conserving process and, if augmented by the application of the PEMF, could help explain the findings.

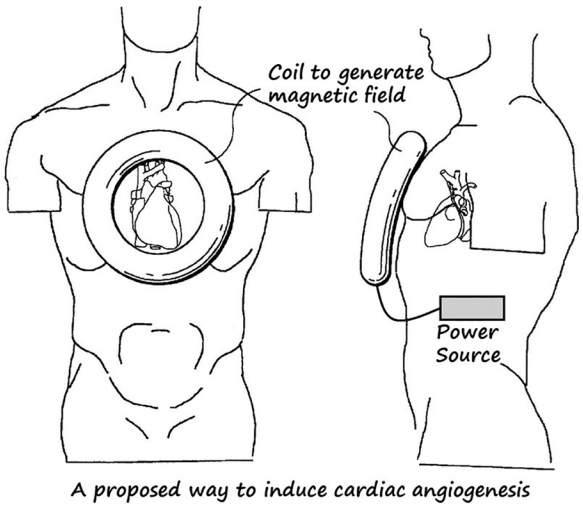

FIGURE 7.9 Illustrating a proposed method for portable cardiac electromagnetic therapy.

Further insight into a potential linkage between magnetic fields, cardiac K_{ATP} channels, and Ca^{++} currents emerges from studies of rat cardiomyocytes in which cultured cells were exposed for 30 min (16 Hz, 40 nT) and Ca^{++} transients measured every 5 min during exposure (Fixler, Yitzhaki et al. 2012). Exposure was associated with a decrease in peak Ca^{++} transients that, based on K_{ATP} channel blocking agent effects, was concluded to be most likely dependent on field-induced changes in these channels. This mechanistic concept, regarding field-induced alterations in Ca^{++} dynamics, follows elements of general theoretical and applied thoughts and findings of several of the pioneers in the field including Arthur Pilla (Pilla 1974, Pilla and Markov 1994, Pilla 2013), Abraham Liboff and Bruce Mcleod (McLeod and Liboff 1986, Smith, McLeod et al. 1987, Liboff and Parkinson 1991, McLeod, Liboff et al. 1992, Liboff 1997, Vincze, Szasz et al. 2008, Liboff, Poggi et al. 2017), Carl Blackman (Blackman, Benane et al. 1975, 1982, 1988), and others including the esteemed editor of this volume, Marko Markov.

Vascular Targets

Although there has been little specific work related to coronary vessels, it is likely that information gained from biomagnetic work on peripheral blood vessels will impact future aspects of cardiac applications. There have been many investigations of static magnetic field impacts on biological systems to assess potential impacts of magnets of various designs and magnetic fields of various patterns and intensities on blood cells, vessels, and blood flow. A view held by some is that static magnet field effects are most evident when applied to physiological states that are deviated from normal. Work done by our group using static magnets on healthy persons has for the most part been consistent with that concept. In one example, skin blood flow was measured on the index finger when one hand was exposed to local

magnetic fields of about 50 mT at the thenar eminence and about 40 mT along the finger for 36 min with corresponding shams simultaneously applied to the other hand (Mayrovitz, Groseclose et al. 2001). The difference between the sham and magnet flows was not significant at any time point whether measured with laser Doppler flowmetry or laser Doppler imaging. Other experiments did not detect a flow effect (Mayrovitz, Groseclose et al. 2005), whereas experiments using a different magnet intensity showed a clear decrease in skin blood flow (Mayrovitz and Groseclose 2005a). Figures 7.10 and 7.11 illustrate the type of arrangements and data obtained in such experiments. In Figure 7.10 is shown laser Doppler blood flow measurement in the middle finger at two sites with the finger gently resting on a neodymium magnet with a surface field of 0.4 T. The blood flow recordings are shown when the finger is first resting on a sham magnet for 16 min followed by its resting on the magnet for 32 min. Figure 7.11 illustrates simultaneous skin blood flow measurements while one finger (F2) rests on a magnet and another (F4) rests on a sham-like surface. Such protocols have both fingers first resting on the sham, and then one of the shams is replaced with the magnet. The recorded blood flow data shows how similar the skin blood flow in the fingers is and the absence of a clearly observable effect of the magnet in this case.

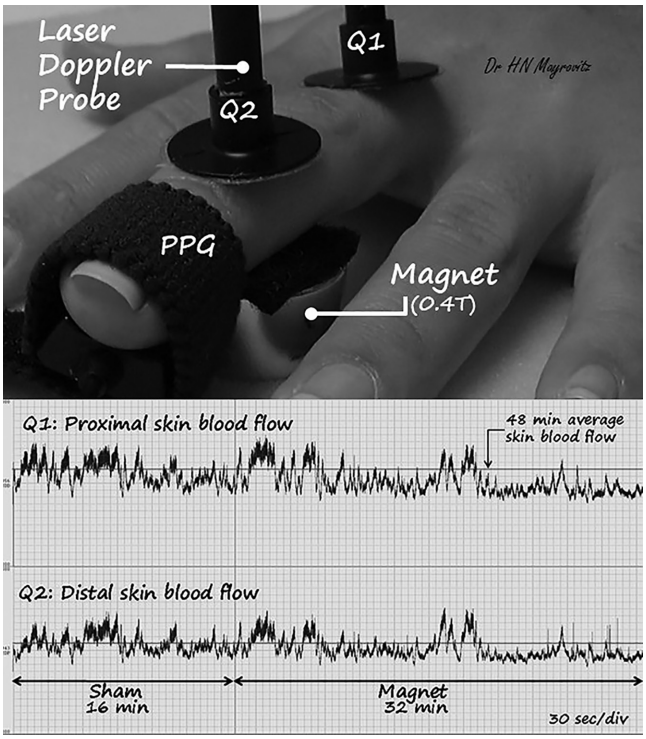

FIGURE 7.10 Illustrating skin blood flow at two points on the same finger exposed to a SMF.

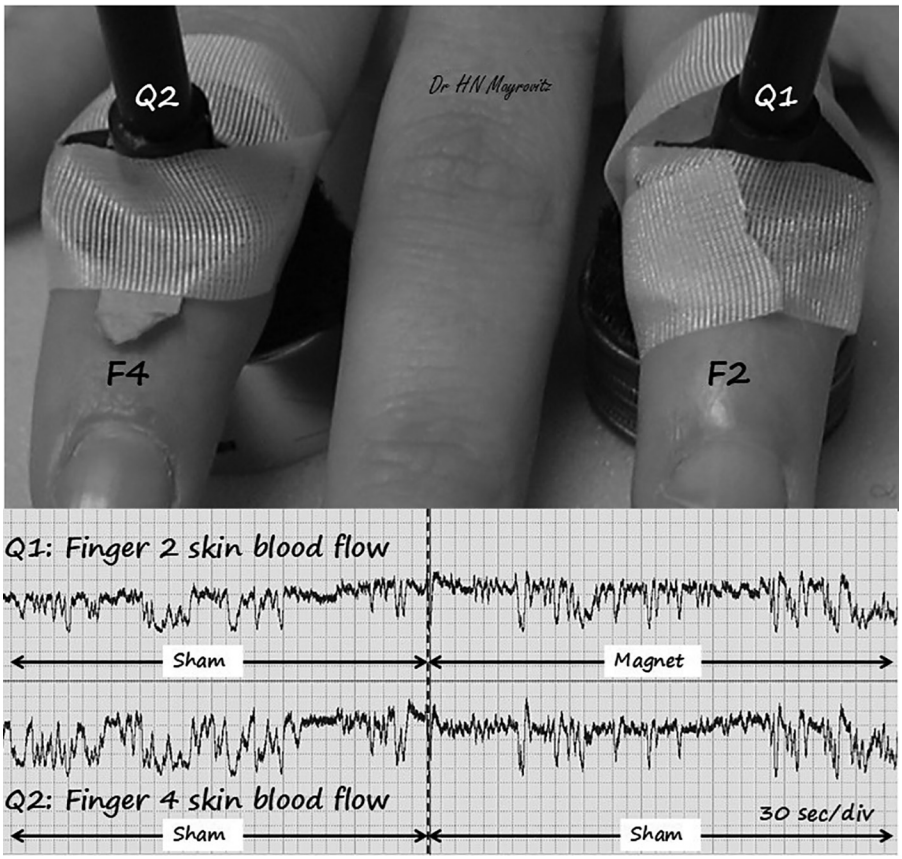

FIGURE 7.11 Illustrating finger pulses measured with photoplethysmography (PPG) with fingers exposed to a vertical SMF or SHAM magnets. The decrease in the PPG signal is due to vasoconstriction attributed to deep inspiration not the magnetic field.

Figure 7.12 illustrates a fully instrumented method using simultaneous skin blood flow, skin temperature, and photoplethysmography (PPG) using the same finger on opposite hands in which one finger is exposed to a magnet and the other exposed to a sham. From the point of view of set-up and subject convenience, this is a recommended approach. The data shown is the PPG signal demonstrating the similarity of these two hand sides in this parameter. The dramatic decrease in both PPG signals is due to a rapid inhalation taken by the subject. This type of response is due to vasoconstriction caused by the so-called inspiratory gasp (Mayrovitz and Groseclose 2002a,b, 2005b). An example of another configuration is illustrated in Figure 7.13 that depicts skin blood flow recorded in the middle finger before and during exposure to a magnet with a surface field of 0.4 T arranged with the field parallel to the long axis of the finger. The change in the flow pattern over the first 3 min of exposure is noted but not yet explained. Additional descriptions and further details of these types of vascular–magnetic dynamics may be found in several book chapters (Mayrovitz 2004, 2015, 2017).

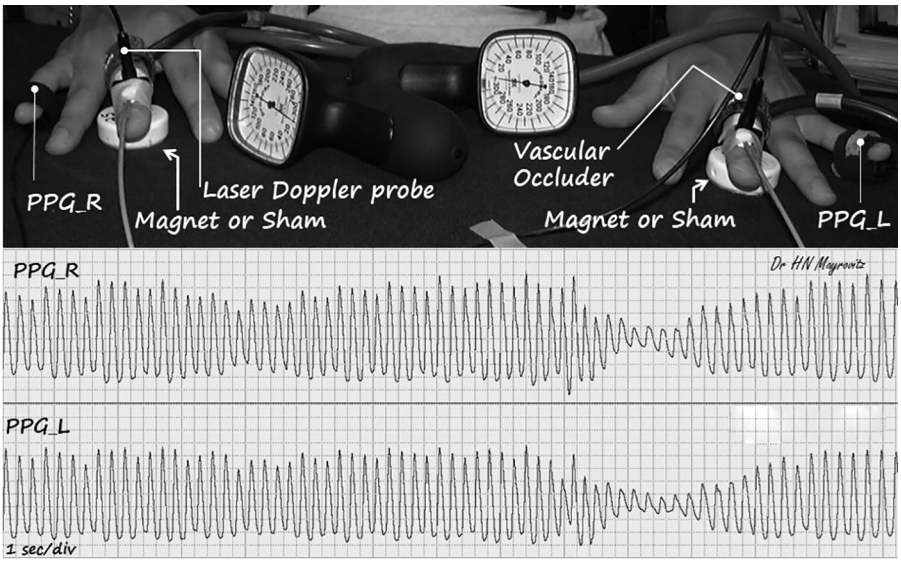

FIGURE 7.12 Illustrating simultaneous finger skin blood flow on two different fingers of the same hand while exposed to a magnet or a sham.

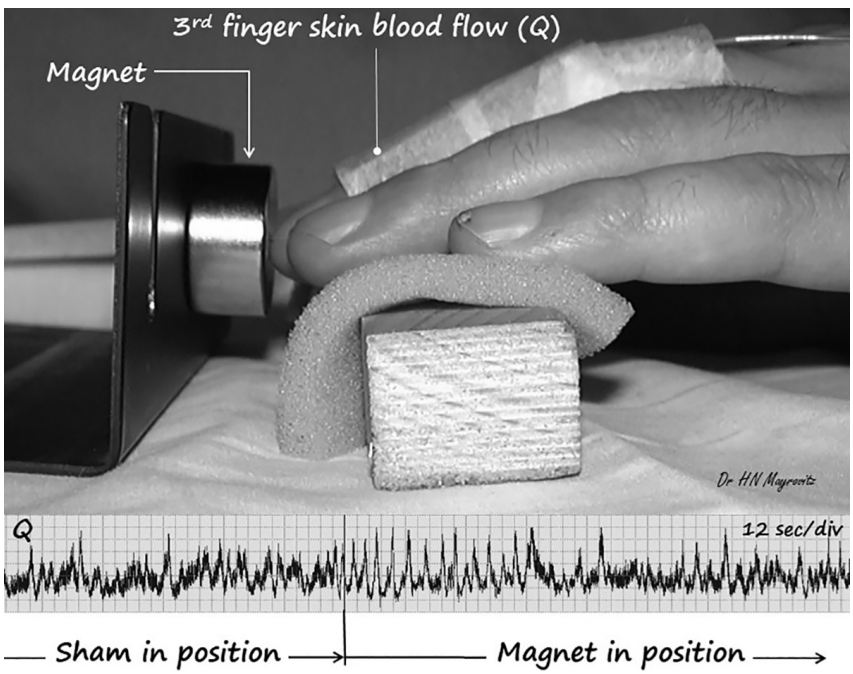

FIGURE 7.13 Illustrating finger dorsum skin blood flow when the finger is exposed to high field intensity acting mainly longitudinally along the finger.

The impact of time-varying magnetic fields as it relates to possible induced changes in vascular-related processes has also been investigated in our laboratory. One example of this is illustrated in Figure 7.14 that illustrates a method to produce pulsating magnetic fields with varying frequency and intensities at skin target sites. At a fixed rotation speed of the turn table, the number of impulses experienced at the target depends on the number of magnets placed on the surface. The example shows an excitation of 20 magnetic pulses per minute with skin blood flow shown prior to and during the exposure. A slight decrease in skin blood flow of both fingers was noted in this experiment with initiation of pulse exposure.

Another work in our laboratory has focused on the potential utility of bioelectromagnetics for lymphatic vessels especially as it relates to the clinical condition known as lymphedema. One such important application is the use of electromagnetic tissue properties to evaluate the tissue dielectric constant (TDC) to assess the

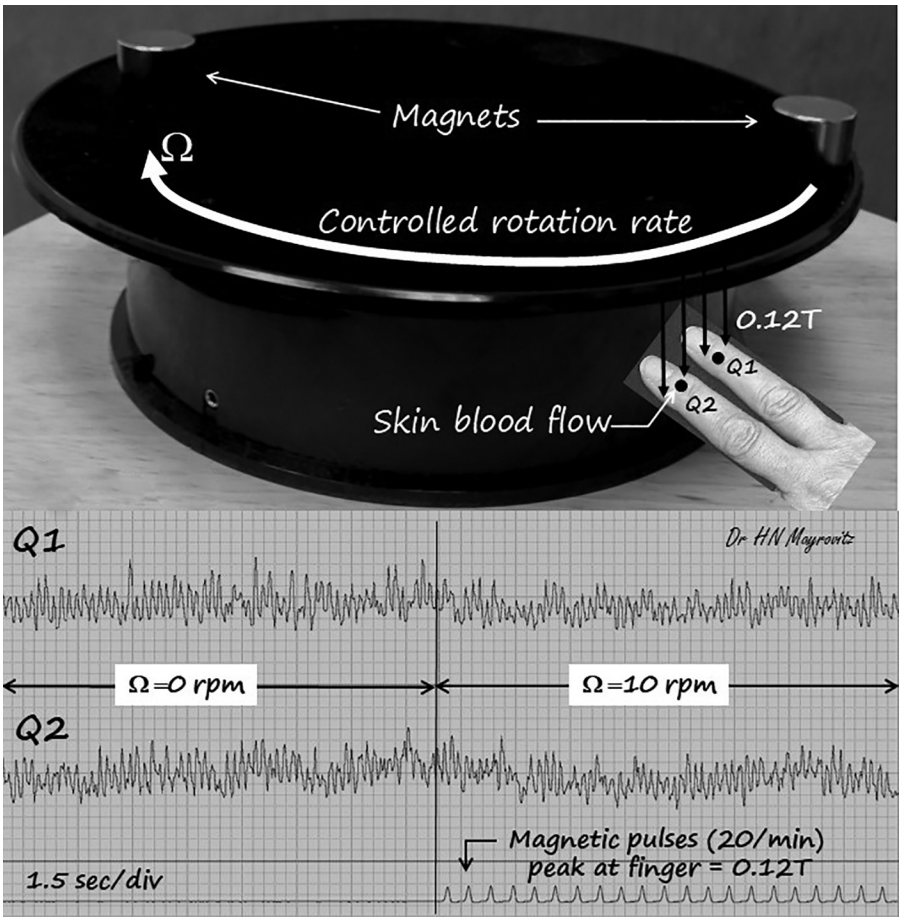

FIGURE 7.14 Illustrating finger skin blood flow while exposed to a time varying magnetic field associated with rotating magnets.

early presence of lymphedema and to track its natural or treatment-related lymphedema (Mayrovitz, Weingrad et al. 2014, 2015, Mayrovitz, Mikulka et al. 2018, Mayrovitz and Weingrad 2018). Other clinical applications have shown utility in the assessment of tissue edema in persons with diabetes (Mayrovitz, McClymont et al. 2013, Mayrovitz, Volosko et al. 2017) and as a possible index of the onset of lower-extremity edema in congestive heart failure. Figure 7.15 illustrates the utilization of this method in which a 300 MHz signal is used to interrogate the tissue in contact with the probe and the reflected electromagnetic energy is used to calculate the TDC as a direct index of tissue water and its change. The measurement principle is based on that of the open-ended coaxial line (Stuchly, Athey et al. 1982, Aimoto and Matsumoto 1996, Gabriel, Lau et al. 1996). Panels A through D illustrate typical measurement sites using two different size probes with the larger probe measuring to a greater depth. The bar graph in Figure 7.15 shows TDC values for different depth measurements on the thigh made 1 month apart in a group of volunteer subjects. It demonstrates that TDC values at certain sites decrease with increasing depth due to decreasing water content but may remain stable over time.

An additional application relevant to lymphedema is the possibility of using PEMF to assist with therapy. Work in this area relates to the potential effects of PEMF on both vascular and lymphatic networks. One study, using PEMF to modulate a

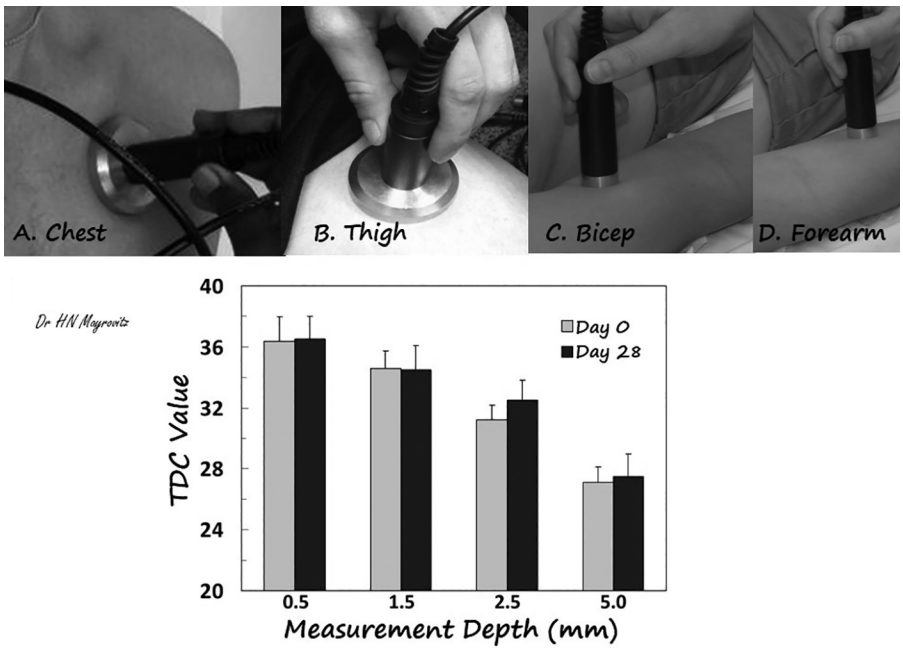

FIGURE 7.15 Illustrating the use of a 300 Hz probe to measure the skin-to-fat tissue dielectric constant (TDC) at various tissue depths. This is a unique application of bioelectromagnetic fields to measure tissue properties mainly related to changes in water content especially in cases of edema and lymphedema.

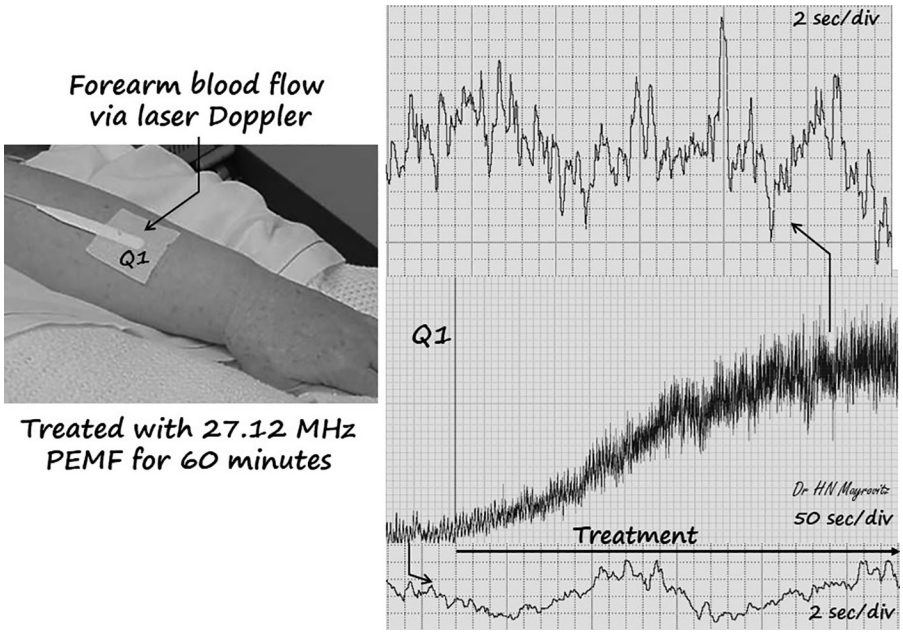

FIGURE 7.16 Illustrating the effect of PEMF at 27.12 MHz in patients with arm lymphedema as a result of treatment for breast cancer. The top and bottom parts of the figure show a magnified expanded time scale corresponding to the time points shown by the arrows. The elevated blood flow during treatment is significant.

27.12 MHz carrier, showed significant improvement in women with breast-cancer-related lymphedema (Mayrovitz, Sims et al. 2002). Figure 7.16 shows a typical blood flow response. Though not measured, it is believed that lymphatic flow may proceed in a similar way. One theory herein offered is that the increased blood pulsations, shown occurring with progressive treatment time, serve as stimuli to promote augmentation of lymphatic emptying thereby accounting for the observed reduction in lymphedema. Further research in this area is needed to verify and further extend this approach.

REFERENCES

Abe, K., H. Hamada, Y. J. Chen, A. Abe, H. Watanabe, Y. Fujiki, H. Yoshikawa, T. Murakami and H. Horigome (2005). "Successful management of supraventricular tachycardia in a fetus using fetal magnetocardiography." *Fetal Diagn Ther* **20**(5): 459–462.

Aharonovich, Y., M. Scheinowitz and S. Zlochiver (2016). "Cardiac KATP channel modulation by 16Hz magnetic fields - A theoretical study." *Conf Proc IEEE Eng Med Biol Soc* **2016**: 161–164.

Aimoto, A. and T. Matsumoto (1996). "Noninvasive method for measuring the electrical properties of deep tissues using an open-ended coaxial probe." *Med Eng Phys* **18**(8): 641–646.

Alabdulgader, A., R. McCraty, M. Atkinson, Y. Dobyns, A. Vainoras, M. Ragulskis and V. Stolc (2018). "Long-term study of heart rate variability responses to changes in the solar and geomagnetic environment." *Sci Rep* **8**(1): 2663.

Bali, R. and U. Awasthi (2011). "Mathematical model of blood flow in small blood vessel in the presence of magnetic field." *Applied Mathematics* **2**: 264–269.

Barach, J. P. and J. P. Wikswo, Jr. (1994). "Magnetic fields from simulated cardiac action currents." *IEEE Trans Biomed Eng* **41**(10): 969–974.

Barisano, G., F. Sepehrband, S. Ma, K. Jann, R. Cabeen, D. J. Wang, A. W. Toga and M. Law (2018). "Clinical 7 T MRI: Are we there yet? A review about magnetic resonance imaging at ultra-high field." *Br J Radiol* **92**(1094): 20180492.

Barry, R. L., S. J. Vannesjo, S. By, J. C. Gore and S. A. Smith (2018). "Spinal cord MRI at 7T." *Neuroimage* **168**: 437–451.

Barry, W. H., W. M. Fairbank, D. C. Harrison, K. L. Lehrman, J. A. Malmivuo and J. P. Wikswo, Jr. (1977). "Measurement of the human magnetic heart vector." *Science* **198**(4322): 1159–1162.

Barzelai, S., A. Dayan, M. S. Feinberg, R. Holbova, S. Laniado and M. Scheinowitz (2009). "Electromagnetic field at 15.95–16 Hz is cardio protective following acute myocardial infarction." *Ann Biomed Eng* **37**(10): 2093–2104.

Batie, M., S. Bitant, J. F. Strasburger, V. Shah, O. Alem and R. T. Wakai (2018). "Detection of fetal arrhythmia using optically-pumped magnetometers." *JACC Clin Electrophysiol* **4**(2): 284–287.

Baule, G. and R. McFee (1963). "Detection of the magnetic field of the heart." *Am Heart J* **66**: 95–96.

Beischer, D. E. and J. C. Knepton, Jr. (1964). "Influence of strong magnetic fields on the electrocardiogram of squirrel monkeys (Saimiri Sciureus)." *Aerosp Med* **35**: 939–944.

Blackman, C. F., S. G. Benane, D. J. Elliott, D. E. House and M. M. Pollock (1988). "Influence of electromagnetic fields on the efflux of calcium ions from brain tissue in vitro: a three-model analysis consistent with the frequency response up to 510 Hz." *Bioelectromagnetics* **9**(3): 215–227.

Blackman, C. F., S. G. Benane, L. S. Kinney, W. T. Joines and D. E. House (1982). "Effects of ELF fields on calcium-ion efflux from brain tissue in vitro." *Radiat Res* **92**(3): 510–520.

Blackman, C. F., S. G. Benane, C. M. Weil and J. S. Ali (1975). "Effects of nonionizing electromagnetic radiation on single-cell biologic systems." *Ann N Y Acad Sci* **247**: 352–366.

Brockmeier, K., L. Schmitz, J. D. Bobadilla Chavez, M. Burghoff, H. Koch, R. Zimmermann and L. Trahms (1997). "Magnetocardiography and 32-lead potential mapping: repolarization in normal subjects during pharmacologically induced stress." *J Cardiovasc Electrophysiol* **8**(6): 615–626.

Cabrerizo, M., A. Cabrera, J. O. Perez, J. de la Rua, N. Rojas, Q. Zhou, A. Pinzon-Ardila, S. M. Gonzalez-Arias and M. Adjouadi (2014). "Induced effects of transcranial magnetic stimulation on the autonomic nervous system and the cardiac rhythm." *Sci World J* **2014**: 349718.

Chakeres, D. W., A. Kangarlu, H. Boudoulas and D. C. Young (2003). "Effect of static magnetic field exposure of up to 8 Tesla on sequential human vital sign measurements." *J Magn Reson Imaging* **18**(3): 346–352.

Chen, I. H. and S. Saha (1984). "Analysis of an intensive magnetic filed on blood flow." *J Bioelectricity* **3**(1 & 2): 293–298.

Chen, P. S., L. S. Chen, M. C. Fishbein, S. F. Lin and S. Nattel (2014). "Role of the autonomic nervous system in atrial fibrillation: Pathophysiology and therapy." *Circ Res* **114**(9): 1500–1515.

Cohen, D. and L. A. Kaufman (1975). "Magnetic determination of the relationship between the S-T segment shift and the injury current produced by coronary artery occlusion." *Circ Res* **36**(3): 414–424.

Cohen, D., J. C. Norman, F. Molokhia and W. Hood, Jr. (1971). "Magnetocardiography of direct currents: S-T segment and baseline shifts during experimental myocardial infarction." *Science* **172**(3990): 1329–1333.

Cohen, D., P. Savard, R. D. Rifkin, E. Lepeschkin and W. E. Strauss (1983). "Magnetic measurement of S-T and T-Q segment shifts in humans. Part II: Exercise-induced S-T segment depression." *Circ Res* **53**(2): 274–279.

Coulton, L. A., A. T. Barker, J. E. Van Lierop and M. P. Walsh (2000). "The effect of static magnetic fields on the rate of calcium/calmodulin-dependent phosphorylation of myosin light chain." *Bioelectromagnetics* **21**(3): 189–196.

Czapski, P., C. Ramon, L. L. Huntsman, G. H. Bardy and Y. Kim (1996). "Effects of tissue conductivity variations on the cardiac magnetic fields simulated with a realistic heart-torso model." *Phys Med Biol* **41**(8): 1247–1263.

Delle Monache, S., A. Angelucci, P. Sanita, R. Iorio, F. Bennato, F. Mancini, G. Gualtieri and R. C. Colonna (2013). "Inhibition of angiogenesis mediated by extremely low-frequency magnetic fields (ELF-MFs)." *PLoS One* **8**(11): e79309.

Derkacz, A., J. Gawrys, K. Gawrys, M. Podgorski, A. Magott-Derkacz, R. Poreba and A. Doroszko (2018). "Effect of electromagnetic field accompanying the magnetic resonance imaging on human heart rate variability - a pilot study." *Int J Inj Contr Saf Promot* **25**(2): 229–231.

DiFrancesco, D. (2010). "The role of the funny current in pacemaker activity." *Circ Res* **106**(3): 434–446.

Ellervik, C., C. Roselli, I. E. Christophersen, A. Alonso, M. Pietzner, C. M. Sitlani, S. Trompet, D. E. Arking, B. Geelhoed, X. Guo, M. E. Kleber, H. J. Lin, H. Lin, P. MacFarlane, E. Selvin, C. Shaffer, A. V. Smith, N. Verweij, S. Weiss, A. R. Cappola, M. Dorr, V. Gudnason, S. Heckbert, S. Mooijaart, W. Marz, B. M. Psaty, P. M. Ridker, D. Roden, D. J. Stott, H. Volzke, E. J. Benjamin, G. Delgado, P. Ellinor, G. Homuth, A. Kottgen, J. W. Jukema, S. A. Lubitz, S. Mora, M. Rienstra, J. I. Rotter, M. B. Shoemaker, N. Sotoodehnia, K. D. Taylor, P. van der Harst, C. M. Albert and D. I. Chasman (2019). "Assessment of the relationship between genetic determinants of thyroid function and atrial fibrillation: A Mendelian randomization study." *JAMA Cardiol* **4**(2): 144–152.

Escalona-Vargas, D., H. T. Wu, M. G. Frasch and H. Eswaran (2018). "A comparison of five algorithms for fetal magnetocardiography signal extraction." *Cardiovasc Eng Technol* **9**(3): 483–487.

Fixler, D., S. Yitzhaki, A. Axelrod, T. Zinman and A. Shainberg (2012). "Correlation of magnetic AC field on cardiac myocyte Ca(2+) transients at different magnetic DC levels." *Bioelectromagnetics* **33**(8): 634–640.

Fujino, K., M. Sumi, K. Saito, M. Murakami, T. Higuchi, Y. Nakaya and H. Mori (1984). "Magnetocardiograms of patients with left ventricular overloading recorded with a second-derivative SQUID gradiometer." *J Electrocardiol* **17**(3): 219–228.

Gabriel, S., R. W. Lau and C. Gabriel (1996). "The dielectric properties of biological tissues: II. Measurements in the frequency range 10 Hz to 20 GHz." *Phys Med Biol* **41**(11): 2251–2269.

Gapelyuk, A., A. Schirdewan, R. Fischer and N. Wessel (2010). "Cardiac magnetic field mapping quantified by Kullback-Leibler entropy detects patients with coronary artery disease." *Physiol Meas* **31**(10): 1345–1354.

Gapelyuk, A., N. Wessel, R. Fischer, U. Zacharzowsky, L. Koch, D. Selbig, H. Schutt, B. Sawitzki, F. C. Luft, R. Dietz and A. Schirdewan (2007). "Detection of patients with coronary artery disease using cardiac magnetic field mapping at rest." *J Electrocardiol* **40**(5): 401–407.

Geselowitz, D. B. (1973). "Electric and magnetic field of the heart." *Annu Rev Biophys Bioeng* **2**: 37–64.

Geselowitz, D. B. (1979). "Magnetocardiography: An overview." *IEEE Trans Biomed Eng* **26**(9): 497–504.

Geurts, L. J., A. A. Bhogal, J. C. W. Siero, P. R. Luijten, G. J. Biessels and J. J. M. Zwanenburg (2018). "Vascular reactivity in small cerebral perforating arteries with 7T phase contrast MRI - A proof of concept study." *Neuroimage* **172**: 470–477.

Geurts, L. J., J. J. M. Zwanenburg, C. J. M. Klijn, P. R. Luijten and G. J. Biessels (2018). "Higher pulsatility in cerebral perforating arteries in patients with small vessel disease related stroke, a 7T MRI study." *Stroke*: STROKEAHA118022516. doi: 10.1161/STROKEAHA.118.022516.

Ghadimi-Moghadam, A., S. M. J. Mortazavi, A. Hosseini-Moghadam, M. Haghani, S. Taeb, M. A. Hosseini, N. Rastegariyan, F. Arian, L. Sanipour, S. Aghajari, S. A. R. Mortazavi, A. Soofi and M. R. Dizavandi (2018). "Does exposure to static magnetic fields generated by magnetic resonance imaging scanners raise safety problems for personnel?" *J Biomed Phys Eng* **8**(3): 333–336.

Haik, Y., V. Pai and C.-J. C. Chen (2001). "Apparent viscosity of human blood in a high static magnetic field." *J Magn Magn Mater* **225**: 180–186.

Higashi, T., N. Asjoda and T. Takeuchi (1997). "Orientation of blood cells in static magnetic field." *Physica B* **237–238**: 616–620.

Horigome, H., M. I. Takahashi, M. Asaka, S. Shigemitsu, A. Kandori and K. Tsukada (2000). "Magnetocardiographic determination of the developmental changes in PQ, QRS and QT intervals in the foetus." *Acta Paediatr* **89**(1): 64–67.

Hosono, T., M. Shinto, Y. Chiba, A. Kandori and K. Tsukada (2002). "Prenatal diagnosis of fetal complete atrioventricular block with QT prolongation and alternating ventricular pacemakers using multi-channel magnetocardiography and current-arrow maps." *Fetal Diagn Ther* **17**(3): 173–176.

Jarusevicius, G., T. Rugelis, R. McCraty, M. Landauskas, K. Berskiene and A. Vainoras (2018). "Correlation between changes in local earth's magnetic field and cases of acute myocardial infarction." *Int J Environ Res Public Health* **15**(3). doi: 10.3390/ijerph15030399.

Jehenson, P., D. Duboc, T. Lavergne, L. Guize, F. Guerin, M. Degeorges and A. Syrota (1988). "Change in human cardiac rhythm induced by a 2-T static magnetic field." *Radiology* **166**(1 Pt 1): 227–230.

Kandori, A., T. Hosono, Y. Chiba, M. Shinto, S. Miyashita, M. Murakami, T. Miyashita, K. Ogata and K. Tsukada (2003). "Classifying cases of fetal Wolff-Parkinson-White syndrome by estimating the accessory pathway from fetal magnetocardiograms." *Med Biol Eng Comput* **41**(1): 33–39.

Kandori, A., T. Hosono, T. Kanagawa, S. Miyashita, Y. Chiba, M. Murakami, T. Miyashita and K. Tsukada (2002). "Detection of atrial-flutter and atrial-fibrillation waveforms by fetal magnetocardiogram." *Med Biol Eng Comput* **40**(2): 213–217.

Kassab, G. S., J. A. Navia and Y. Huo (2013). Devices, systems and methods for pacing, resynchonization and defibrillation therapy. US Patent 8,396,566. USA, CVDevices. 8396566.

Kawakami, S., H. Takaki, S. Hashimoto, Y. Kimura, T. Nakashima, T. Aiba, K. F. Kusano, S. Kamakura, S. Yasuda and M. Sugimachi (2016). "Utility of high-resolution magnetocardiography to predict later cardiac events in nonischemic cardiomyopathy patients with normal QRS duration." *Circ J* **81**(1): 44–51.

Kiefer-Schmidt, I., M. Lim, H. Preissl, R. Draganova, M. Weiss, H. Abele, K. O. Kagan and J. Henes (2014). "Fetal magnetocardiography (fMCG) to monitor cardiac time intervals in fetuses at risk for isoimmune AV block." *Lupus* **23**(9): 919–925.

Kimura, Y., H. Takaki, Y. Y. Inoue, Y. Oguchi, T. Nagayama, T. Nakashima, S. Kawakami, S. Nagase, T. Noda, T. Aiba, W. Shimizu, S. Kamakura, M. Sugimachi, S. Yasuda, H. Shimokawa and K. Kusano (2017). "Isolated late activation detected by magnetocardiography predicts future lethal ventricular arrhythmic events in patients with arrhythmogenic right ventricular cardiomyopathy." *Circ J* **82**(1): 78–86.

Kinouchi, Y., H. Yamaguchi and T. S. Tenforde (1996). "Theoretical analysis of magnetic field interactions with aortic blood flow." *Bioelectromagnetics* **17**(1): 21–32.

Kolin, A., N. Assali, G. Herrold and R. Jensen (1957). "Electromagnetic determination of regional blood flow in unanesthetized animals." *Proc Natl Acad Sci USA* **43**(6): 527–540.

Koppel, T., I. Vilcane, M. Carlberg, P. Tint, R. Priiman, K. Riisik, H. Haldre and L. Visnapuu (2015). "The effect of static magnetic field on heart rate variability – an experimental study." *Agron Res* **13**(3): 765–774.

Kurokawa, Y., H. Nitta, H. Imai and M. Kabuto (2003). "Can extremely low frequency alternating magnetic fields modulate heart rate or its variability in humans?" *Auton Neurosci* **105**(1): 53–61.

Laniado, S., Z. Kamil and E. Nhaissi (2005). Method and apparatus for non-invasive therapy of cardiovascular ailments using weak pulsed electromagnetic radiation. US Patent 02,22,625 A1.

Li, F., Y. Yuan, Y. Guo, N. Liu, D. Jing, H. Wang and W. Guo (2015). "Pulsed magnetic field accelerate proliferation and migration of cardiac microvascular endothelial cells." *Bioelectromagnetics* **36**(1): 1–9.

Li, S., X. Zhou, L. Yu and H. Jiang (2015). "Low level non-invasive vagus nerve stimulation: a novel feasible therapeutic approach for atrial fibrillation." *Int J Cardiol* **182**: 189–190.

Li, X. and J. V. Rispoli (2019). "Toward 7T breast MRI clinical study: Safety assessment using simulation of heterogeneous breast models in RF exposure." *Magn Reson Med* **81**(2): 1307–1321.

Liboff, A. R. (1997). "Electric-field ion cyclotron resonance." *Bioelectromagnetics* **18**(1): 85–87.

Liboff, A. R. and W. C. Parkinson (1991). "Search for ion-cyclotron resonance in an Na(+)-transport system." *Bioelectromagnetics* **12**(2): 77–83.

Liboff, A. R., C. Poggi and P. Pratesi (2017). "Weak low-frequency electromagnetic oscillations in water." *Electromagn Biol Med* **36**(2): 154–157.

Liu, L. and S. Nattel (1997). "Differing sympathetic and vagal effects on atrial fibrillation in dogs: Role of refractoriness heterogeneity." *Am J Physiol* **273**(2 Pt 2): H805–816.

Loomba, R. S. and R. Arora (2009). "ST elevation myocardial infarction guidelines today: A systematic review exploring updated ACC/AHA STEMI guidelines and their applications." *Am J Ther* **16**(5): e7–e13.

Lu, X. W., L. Du, L. Kou, N. Song, Y. J. Zhang, M. K. Wu and J. F. Shen (2015). "Effects of moderate static magnetic fields on the voltage-gated sodium and calcium channel currents in trigeminal ganglion neurons." *Electromagn Biol Med* **34**(4): 285–292.

March, K. L. (2001). Methods of treating cardiovascular disease by angiogenesis. U.S. Patent 6,200,259.

Markenroth Bloch, K., J. Toger and F. Stahlberg (2018). "Investigation of cerebrospinal fluid flow in the cerebral aqueduct using high-resolution phase contrast measurements at 7T MRI." *Acta Radiol* **59**(8): 988–996.

Markov, M. S. (2010). "Angiogenesis, magnetic fields and 'window effects'." *Cardiology* **117**(1): 54–56.

Mayrovitz, H. N. (2004). Electromagentic linkages in soft tissue wound healing. In P. J. Rosch and M. Markov, *Bioelectric Medicine*. New York, Marcel Dekker: pp. 461–483.

Mayrovitz, H. N. (2015). Electromagnetic fields for soft tissue wound healing. In M. S. Markov, *Electromagnetic Fields in Biology and Medicine*. Boca Raton, FL, CRC Press: pp. 231–251.

Mayrovitz, H. N. (2017). Blood and vascular targets for magnetic dosing. In M. S. Markov, *Dosimetry in Bioelectromagnetics*. Boca Raton, FL, CRC Press: pp. 285–313.

Mayrovitz, H. N. and E. E. Groseclose (2002a). "Inspiration-induced vascular responses in finger dorsum skin." *Microvasc Res* **63**(2): 227–232.

Mayrovitz, H. N. and E. E. Groseclose (2002b). "Neurovascular responses to sequential deep inspirations assessed via laser-Doppler perfusion changes in dorsal finger skin." *Clin Physiol Funct Imaging* **22**(1): 49–54.

Mayrovitz, H. N. and E. E. Groseclose (2005a). "Effects of a static magnetic field of either polarity on skin microcirculation." *Microvasc Res* **69**(1–2): 24–27.

Mayrovitz, H. N. and E. E. Groseclose (2005b). "Inspiration-induced vasoconstrictive responses in dominant versus non-dominant hands." *Clin Physiol Funct Imaging* **25**(2): 69–74.

Mayrovitz, H. N., E. E. Groseclose and D. King (2005). "No effect of 85 mT permanent magnets on laser-Doppler measured blood flow response to inspiratory gasps." *Bioelectromagnetics* **26**(4): 331–335.

Mayrovitz, H. N., E. E. Groseclose, M. Markov and A. A. Pilla (2001). "Effects of permanent magnets on resting skin blood perfusion in healthy persons assessed by laser Doppler flowmetry and imaging." *Bioelectromagnetics* **22**(7): 494–502.

Mayrovitz, H. N., A. McClymont and N. Pandya (2013). "Skin tissue water assessed via tissue dielectric constant measurements in persons with and without diabetes mellitus." *Diabetes Technol Ther* **15**(1): 60–65.

Mayrovitz, H. N., A. Mikulka and D. Woody (2018). "Minimum detectable changes associated with tissue dielectric constant measurements as applicable to assessing lymphedema status." *Lymphat Res Biol* **17**(3): 322–328.

Mayrovitz, H. N., N. Sims and J. M. Macdonald (2002). "Effects of pulsed radio frequency diathermy on postmastectomy arm lymphedema and skin blood flow: A pilot investigation." *Lymphology* **35** (suppl): 353–356.

Mayrovitz, H. N., I. Volosko, B. Sarkar and N. Pandya (2017). "Arm, leg, and foot skin water in persons with diabetes mellitus (DM) in relation to HbA1c assessed by tissue dielectric constant (TDC) technology measured at 300 MHz." *J Diabetes Sci Technol* **11**(3): 584–589.

Mayrovitz, H. N. and D. N. Weingrad (2018). "Tissue dielectric constant ratios as a method to characterize truncal lymphedema." *Lymphology* **51**(3): 125–131.

Mayrovitz, H. N., D. N. Weingrad and S. Davey (2014). "Tissue dielectric constant (TDC) measurements as a means of characterizing localized tissue water in arms of women with and without breast cancer treatment related lymphedema." *Lymphology* **47**(3): 142–150.

Mayrovitz, H. N., D. N. Weingrad and L. Lopez (2015). "Patterns of temporal changes in tissue dielectric constant as indices of localized skin water changes in women treated for breast cancer: a pilot study." *Lymphat Res Biol* **13**(1): 20–32.

McBride, K. K., B. J. Roth, V. Y. Sidorov, J. P. Wikswo and F. J. Baudenbacher (2010). "Measurements of transmembrane potential and magnetic field at the apex of the heart." *Biophys J* **99**(10): 3113–3118.

McCraty, R., M. Atkinson, V. Stolc, A. A. Alabdulgader, A. Vainoras and M. Ragulskis (2017). "Synchronization of human autonomic nervous system rhythms with geomagnetic activity in human subjects." *Int J Environ Res Public Health* **14**(7). doi: 10.3390/ijerph14070770.

McLeod, B. R. and A. R. Liboff (1986). "Dynamic characteristics of membrane ions in multifield configurations of low-frequency electromagnetic radiation." *Bioelectromagnetics* **7**(2): 177–189.

McLeod, B. R., A. R. Liboff and S. D. Smith (1992). "Electromagnetic gating in ion channels." *J Theor Biol* **158**(1): 15–31.

Moraes, E. R., L. O. Murta, O. Baffa, R. T. Wakai and S. Comani (2012). "Linear and nonlinear measures of fetal heart rate patterns evaluated on very short fetal magnetocardiograms." *Physiol Meas* **33**(10): 1563–1583.

Muehsam, D. J. and A. A. Pilla (2009). "A Lorentz model for weak magnetic field bioeffects: part II--secondary transduction mechanisms and measures of reactivity." *Bioelectromagnetics* **30**(6): 476–488.

Nichols, C. G., G. K. Singh and D. K. Grange (2013). "KATP channels and cardiovascular disease: suddenly a syndrome." *Circ Res* **112**(7): 1059–1072.

Nishida, K., T. Datino, L. Macle and S. Nattel (2014). "Atrial fibrillation ablation: Translating basic mechanistic insights to the patient." *J Am Coll Cardiol* **64**(8): 823–831.

Okazaki, M., N. Maeda and T. Shiga (1987). "Effects of an inhomogeneous magnetic field on flowing erythrocytes." *Eur Biophys J* **14**(3): 139–145.

Pagani, M., F. Lombardi, S. Guzzetti, O. Rimoldi, R. Furlan, P. Pizzinelli, G. Sandrone, G. Malfatto, S. Dell'Orto, E. Piccaluga and et al. (1986). "Power spectral analysis of heart rate and arterial pressure variabilities as a marker of sympatho-vagal interaction in man and conscious dog." *Circ Res* **59**(2): 178–193.

Pan, Y., Y. Dong, W. Hou, Z. Ji, K. Zhi, Z. Yin, H. Wen and Y. Chen (2013). "Effects of PEMF on microcirculation and angiogenesis in a model of acute hindlimb ischemia in diabetic rats." *Bioelectromagnetics* **34**(3): 180–188.

Park, C. A., C. K. Kang, Y. B. Kim and Z. H. Cho (2018). "Advances in MR angiography with 7T MRI: From microvascular imaging to functional angiography." *Neuroimage* **168**: 269–278.

Pauza, D. H., V. Skripka, N. Pauziene and R. Stropus (2000). "Morphology, distribution, and variability of the epicardiac neural ganglionated subplexuses in the human heart." *Anat Rec* **259**(4): 353–382.

Pfurtscheller, G., A. Schwerdtfeger, D. Fink, C. Brunner, C. S. Aigner, J. Brito and A. Andrade (2018). "MRI-related anxiety in healthy individuals, intrinsic BOLD oscillations at 0.1 Hz in precentral gyrus and insula, and heart rate variability in low frequency bands." *PLoS One* **13**(11): e0206675.

Pilla, A. A. (1974). "Electrochemical information transfer at living cell membranes." *Ann N Y Acad Sci* **238**: 149–170.

Pilla, A. A. (2013). "Nonthermal electromagnetic fields: From first messenger to therapeutic applications." *Electromagn Biol Med* **32**(2): 123–136.

Pilla, A. A. and M. S. Markov (1994). "Bioeffects of weak electromagnetic fields." *Rev Environ Health* **10**(3–4): 155–169.

Pilla, A. A., D. J. Muehsam, M. S. Markov and B. F. Sisken (1999). "EMF signals and ion/ligand binding kinetics: Prediction of bioeffective waveform parameters." *Bioelectrochem Bioenerg* **48**(1): 27–34.

Plonsey, R. (1972). "Capability and limitations of electrocardiography and magnetocardiography." *IEEE Trans Biomed Eng* **19**(3): 239–244.

Ramon, C. and G. H. Bardy (1992). Leadless Magnetic Cardiac Pacemaker. U.S. Patent 5,170,784.

Reno, V. R. and D. E. Beischer (1966). "Cardiac excitability in high magnetic fields." *Aerosp Med* **37**(12): 1229–1232.

Roberts, J. D. (2019). "Thyroid function and the risk of atrial fibrillation: Exploring potentially causal relationships through Mendelian randomization." *JAMA Cardiol* **4**(2): 97–99.

Roth, B. J. and J. P. Wikswo, Jr. (1986). "Electrically silent magnetic fields." *Biophys J* **50**(4): 739–745.

Salem, J. E., M. B. Shoemaker, L. Bastarache, C. M. Shaffer, A. M. Glazer, B. Kroncke, Q. S. Wells, M. Shi, P. Straub, G. P. Jarvik, E. B. Larson, D. R. Velez Edwards, T. L. Edwards, L. K. Davis, H. Hakonarson, C. Weng, D. Fasel, B. C. Knollmann, T. J. Wang,

J. C. Denny, P. T. Ellinor, D. M. Roden and J. D. Mosley (2019). "Association of thyroid function genetic predictors with atrial fibrillation: A phenome-wide association study and inverse-variance weighted average meta-analysis." *JAMA Cardiol* **4**(2): 136–143.

Savard, P., D. Cohen, E. Lepeschkin, B. N. Cuffin and J. E. Madias (1983). "Magnetic measurement of S-T and T-Q segment shifts in humans. Part I: Early repolarization and left bundle branch block." *Circ Res* **53**(2): 264–273.

Scheinowitz, M., E. Nhaissi, E. Levine and D. Giler (2018). Apparatus for non-invasive therapy of biological tissue using directed magnetic beams. US Patent 10092769 B2.

Schirdewan, A., A. Gapelyuk, R. Fischer, L. Koch, H. Schutt, U. Zacharzowsky, R. Dietz, L. Thierfelder and N. Wessel (2007). "Cardiac magnetic field map topology quantified by Kullback-Leibler entropy identifies patients with hypertrophic cardiomyopathy." *Chaos* **17**(1): 015118.

Schwartz, J. L., D. E. House and G. A. Mealing (1990). "Exposure of frog hearts to CW or amplitude-modulated VHF fields: Selective efflux of calcium ions at 16 Hz." *Bioelectromagnetics* **11**(4): 349–358.

Sert, C., Z. Akti, O. Sirmatel and R. Yilmaz (2010). "An investigation of the heart rate, heart rate variability, cardiac ions, troponin-I and CK-MB in men exposed to 1.5 T constant magnetic fields." *Gen Physiol Biophys* **29**(3): 282–287.

Shaffer, F. and J. P. Ginsberg (2017). "An overview of heart rate variability metrics and norms." *Front Public Health* **5**: 258.

Shin, E. S., J. W. Park and D. S. Lim (2018a). "Magnetocardiography for the diagnosis of non-obstructive coronary artery disease1." *Clin Hemorheol Microcirc* **69**(1–2): 9–11.

Shin, E. S., S. G. Park, A. Saleh, Y. Y. Lam, J. Bhak, F. Jung, S. Morita and J. Brachmann (2018b). "Magnetocardiography scoring system to predict the presence of obstructive coronary artery disease." *Clin Hemorheol Microcirc* **70**(4): 365–373.

Shirai, Y., K. Hirao, T. Shibuya, S. Okawa, Y. Hasegawa, Y. Adachi, K. Sekihara and S. Kawabata (2018). "Magnetocardiography using a magnetoresistive sensor array." *Int Heart J* **60**(1): 50–54.

Smith, F. E., P. Langley, P. van Leeuwen, B. Hailer, L. Trahms, U. Steinhoff, J. P. Bourke and A. Murray (2006). "Comparison of magnetocardiography and electrocardiography: a study of automatic measurement of dispersion of ventricular repolarization." *Europace* **8**(10): 887–893.

Smith, S. D., B. R. McLeod, A. R. Liboff and K. Cooksey (1987). "Calcium cyclotron resonance and diatom mobility." *Bioelectromagnetics* **8**(3): 215–227.

Sorbo, A. R., G. Lombardi, L. La Brocca, G. Guida, R. Fenici and D. Brisinda (2018). "Unshielded magnetocardiography: Repeatability and reproducibility of automatically estimated ventricular repolarization parameters in 204 healthy subjects." *Ann Noninvasive Electrocardiol* **23**(3): e12526.

Stavrakis, S. and S. Po (2017). "Ganglionated plexi ablation: Physiology and clinical applications." *Arrhythm Electrophysiol Rev* **6**(4): 186–190.

Stingl, K., H. Paulsen, M. Weiss, H. Preissl, H. Abele, R. Goelz and A. Wacker-Gussmann (2013). "Development and application of an automated extraction algorithm for fetal magnetocardiography - normal data and arrhythmia detection." *J Perinat Med* **41**(6): 725–734.

Stratbucker, R. A., C. M. Hyde and S. E. Wixson (1963). "The magnetocardiogram--A new approach to the fields surrounding the heart." *IEEE Trans Biomed Eng* **10**: 145–149.

Strelczyk, D., M. E. Eichhorn, S. Luedemann, G. Brix, M. Dellian, A. Berghaus and S. Strieth (2009). "Static magnetic fields impair angiogenesis and growth of solid tumors in vivo." *Cancer Biol Ther* **8**(18): 1756–1762.

Stuchly, M. A., T. W. Athey, G. M. Samaras and G. E. Taylor (1982). "Measurement of radio frequency permittivity of biological tissues with an open-ended coaxial line: Part II - Experimental results." *IEEE Trans Microwave Therory Tech* **30**(1): 87–92.

Sud, V. K. and G. S. Sekhon (1989). "Blood flow through the human arterial system in the presence of a steady magnetic field." *Phys Med Biol* **34**(7): 795–805.

Takeuchi, T., T. Mizuno, T. Higashi, A. Yamagishi and M. Date (1995). "Orientation of red blood cells in high magnetic filed." *J Magn Magn Mater* **140–144**: 1462–1463.

Tao, P., X. Wu, L. Zhao, F. Wang, Q. Xia, Y. Peng and B. Gao (2017). "[Effect of high-intensity alternating magnetic field on viscosity of sheep blood]." *Zhong Nan Da Xue Xue Bao Yi Xue Ban* **42**(12): 1395–1400.

Tao, R. and K. Huang (2011). "Reducing blood viscosity with magnetic fields." *Phys Rev E Stat Nonlin Soft Matter Phys* **84**(1 Pt 1): 011905.

Tao, R., S. Zhang, X. Huang, M. Tao, J. Ma, S. Ma, C. Zhang, T. Zhang, F. Tang, J. Lu, C. Shen and X. Xie (2018). "Magnetocardiography based ischemic heart disease detection and localization using machine learning methods." *IEEE Trans Biomed Eng* **66**(6): 1658–1667.

Tasic, T., D. M. Djordjevic, S. R. De Luka, A. M. Trbovich and N. Japundzic-Zigon (2017). "Static magnetic field reduces blood pressure short-term variability and enhances baroreceptor reflex sensitivity in spontaneously hypertensive rats." *Int J Radiat Biol* **93**(5): 527–534.

Van Hare, G. F. (2013). "Magnetocardiography in the diagnosis of fetal arrhythmias." *Heart Rhythm* **10**(8): 1199–1200.

Van Leeuwen, P., B. Hailer, S. Lange, A. Klein, D. Geue, K. Seybold, C. Poplutz and D. Gronemeyer (2008). "Quantification of cardiac magnetic field orientation during ventricular de- and repolarization." *Phys Med Biol* **53**(9): 2291–2301.

Vincze, G., A. Szasz and A. R. Liboff (2008). "New theoretical treatment of ion resonance phenomena." *Bioelectromagnetics* **29**(5): 380–386.

Wacker-Gussmann, A., H. Paulsen, K. Stingl, J. Braendle, R. Goelz and J. Henes (2014). "Atrioventricular conduction delay in the second trimester measured by fetal magnetocardiography." *J Immunol Res* **2014**: 753953.

Walleczek, J. and T. F. Budinger (1992). "Pulsed magnetic field effects on calcium signaling in lymphocytes: dependence on cell status and field intensity." *FEBS Lett* **314**(3): 351–355.

Wang, Y., M. K. Hensley, A. Tasman, L. Sears, M. F. Casanova and E. M. Sokhadze (2016). "Heart rate variability and skin conductance during repetitive TMS course in children with autism." *Appl Psychophysiol Biofeedback* **41**(1): 47–60.

Wang, Z., P. Yang, H. Xu, A. Qian, L. Hu and P. Shang (2009). "Inhibitory effects of a gradient static magnetic field on normal angiogenesis." *Bioelectromagnetics* **30**(6): 446–453.

Watanabe, S. and S. Yamada (2008). "Magnetocardiography in early detection of electromagnetic abnormality in ischemic heart disease." *J Arrhythmia* **24**: 4–17.

Wikswo, J. P., Jr. (1980). "Noninvasive magnetic detection of cardiac mechanical activity: Theory." *Med Phys* **7**(4): 297–306.

Wikswo, J. P., Jr., J. E. Opfer and W. M. Fairbank (1980). "Noninvasive magnetic detection of cardiac mechanical activity: Experiments." *Med Phys* **7**(4): 307–314.

Woods, C. E. and J. Olgin (2014). "Atrial fibrillation therapy now and in the future: drugs, biologicals, and ablation." *Circ Res* **114**(9): 1532–1546.

Yamaguchi, Y., M. Wada, H. Sato, H. Nagasawa, S. Koyama, Y. Takahashi, T. Kawanami and T. Kato (2015). "Impact of nocturnal heart rate variability on cerebral small-vessel disease progression: a longitudinal study in community-dwelling elderly Japanese." *Hypertens Res* **38**(8): 564–569.

Yoon, D., S. Biswal, B. Rutt, A. Lutz and B. Hargreaves (2018). "Feasibility of 7T MRI for imaging fascicular structures of peripheral nerves." *Muscle Nerve* **57**(3): 494–498.

Yoshida, K., K. Ogata, T. Inaba, Y. Nakazawa, Y. Ito, I. Yamaguchi, A. Kandori and K. Aonuma (2015). "Ability of magnetocardiography to detect regional dominant frequencies of atrial fibrillation." *J Arrhythm* **31**(6): 345–351.

Yoshida, T., A. Yoshino, Y. Kobayashi, M. Inoue, K. Kamakura and S. Nomura (2001). "Effects of slow repetitive transcranial magnetic stimulation on heart rate variability according to power spectrum analysis." *J Neurol Sci* **184**(1): 77–80.

Young, W. (1969). Magnetic field and in situ acetylcholinesterase in the vagal heart system. In M. Barnothy, *Biological Effects of Magnetic Fields*, 2. New York, Plenum Press: pp. 79–102.

Yu, S., B. D. Van Veen and R. T. Wakai (2013). "Detection of T-wave alternans in fetal magnetocardiography using the generalized likelihood ratio test." *IEEE Trans Biomed Eng* **60**(9): 2393–2400.

Yuan, Y., L. Wei, F. Li, W. Guo, W. Li, R. Luan, A. Lv and H. Wang (2010). "Pulsed magnetic field induces angiogenesis and improves cardiac function of surgically induced infarcted myocardium in Sprague-Dawley rats." *Cardiology* **117**(1): 57–63.

Zhao, Y. L., J. C. Yang and Y. H. Zhang (2008). "Effects of magnetic fields on intracellular calcium oscillations." *Conf Proc IEEE Eng Med Biol Soc* **2008**: 2124–2127.

Zhuravlev, Y. E., D. Rassi, A. A. Mishin and S. J. Emery (2002). "Dynamic analysis of beat-to-beat fetal heart rate variability recorded by SQUID magnetometer: quantification of sympatho-vagal balance." *Early Hum Dev* **66**(1): 1–10.

Žiubrytė, G., G. Jaruševičius, J. Jurjonaite, M. Landauskas, R. McCraty and A. Vainoras (2018a). "Correlations between acute atrial fibrillation and local earth magnetic field strength." *J Complexity Health Sci* **1**(2): 31–41.

Žiubrytė, G., G. Jaruševičius, M. Landauskas, R. McCraty and A. Vainoras (2018b). "The local earth magnetic field changes impact on weekly hospitalization due to unstable angina pectoris." *J Complexity Health Sci* **1**(1): 16–25.